Bicyclo[2.2.0]hexene (BCH): A Multimodal Mechanophore with Force-Governed Chemoselectivity

Shihao Ding[1‡], Wenkai Wang[2‡], Anne Germann[3‡], Yiting Wei[1], Tianyi Du[1], Jan Meisner[3]*, Rong Zhu[2]*, Yun Liu[1]*

Addresses: [1]Beijing National Laboratory for Molecular Sciences, Center for Soft Matter Science and Engineering, Key Laboratory of Polymer Chemistry and Physics of Ministry of Education, and College of Chemistry and Molecular Engineering, Peking University, Beijing, 100871, China. [2]Beijing National Laboratory for Molecular Sciences, Key Laboratory of Bioorganic Chemistry and Molecular Engineering of Ministry of Education, and College of Chemistry and Molecular Engineering, Peking University, Beijing, 100871, China. [3]Institute for Physical Chemistry, Faculty of Mathematics and Natural Sciences, Heinrich Heine University Düsseldorf, Düsseldorf, 40225, Germany.

‡These authors contributed equally to this work.

*Corresponding author. Email: meisner@hhu.de (J.M.); rongzhu@pku.edu.cn (R.Z.); yun.liu@pku.edu.cn (Y.L.)

Abstract (198/250 words)

The identity of reactive sites in a molecule and the selectivity between them in chemical transformations depends on applied reagents and external drives. Polymer mechanochemistry has been an enabling tool in accessing chemical reactivity and reaction pathways that are distinctive from the thermal counterparts. However, mechanochemical selectivity, i.e., activation of multiple unique reaction pathways from the same mechanophore, remains elusive. Here, we report the design of bicyclo[2.2.0]hexene (BCH) as a multimodal mechanophore to leverage its structural simplicity and relatively low molecular symmetry to demonstrate the idea of force-governed chemoselectivity. Upon changing the attachment points of pendant polymer chains, different C–C bonds in bicyclo[2.2.0]hexene are specifically activated via sonication by externally applied force. Extensive experimental characterization confirms that each mode of activation results in a unique reaction, entailing retro-[2+2] cycloreversion, 1,3-allylic migration, and 4π-electrocyclic ring-opening reactions, respectively. Control experiments with small-molecule analogues reveal that observed chemoselectivity of BCH regioisomers is only possible with mechanical force. Theoretical studies further elucidate that the changes of substitution have minimal impact on the potential energy surface of parent BCH. The mechanochemical bond-specific activation is a result of selective and effective coupling of force to the targeted C–C bonds in each mode.

INTRODUCTION

Chemical reactivity of a molecule depends on the nature of its energy landscape. The ability to select one reactive site over the other competitive sites on the same landscape allows chemists to perform highly chemoselective transformations on complex organic molecules. In recent years, interest grows on using physical approaches to alter chemoselectivity by manipulating molecular vibrations.[1-3] Strategies using strong laser fields[1,4,5] or vibrational strong coupling of a vacuum cavity have demonstrated new chemoselectivity in small organic molecules.[3,6] Nevertheless, a priori predictions of chemoselectivity accessed by these methods can be complicated by increasing vibrational couplings within a more complex molecule.[5,7] Complementarily, polymer mechanochemistry has been an emerging physicochemical tool to impart unique reactivity, especially in comparison with the thermal counterparts (Figure 1, top box).[8-12] The reactive sites in a mechanochemical reaction is often the chemical bond with the highest susceptibility to change its interatomic distances under stress.[13,14] Lining up multiple mechanochemically reactive sites,[15-17] a.k.a., mechanophores,[18,19] enables gated activation: some reactivity is designed to be revealed after the activation of an initial gating mechanophore,[16,17,20-30] and in some cases a stored length is released to dissipate mechanochemical energy.[31-33] Even from the same transition state, it is possible to control product composition by gauging the branching ratios between different subsequent paths with nonstatistical reaction dynamics.[12,34,35] Here, we wonder, if it is possible to demonstrate chemoselectivity on a given force-modified potential energy surface, thereby achieving several unique reactions within one mechanophore by varying the applied force (Figure 1, central box).

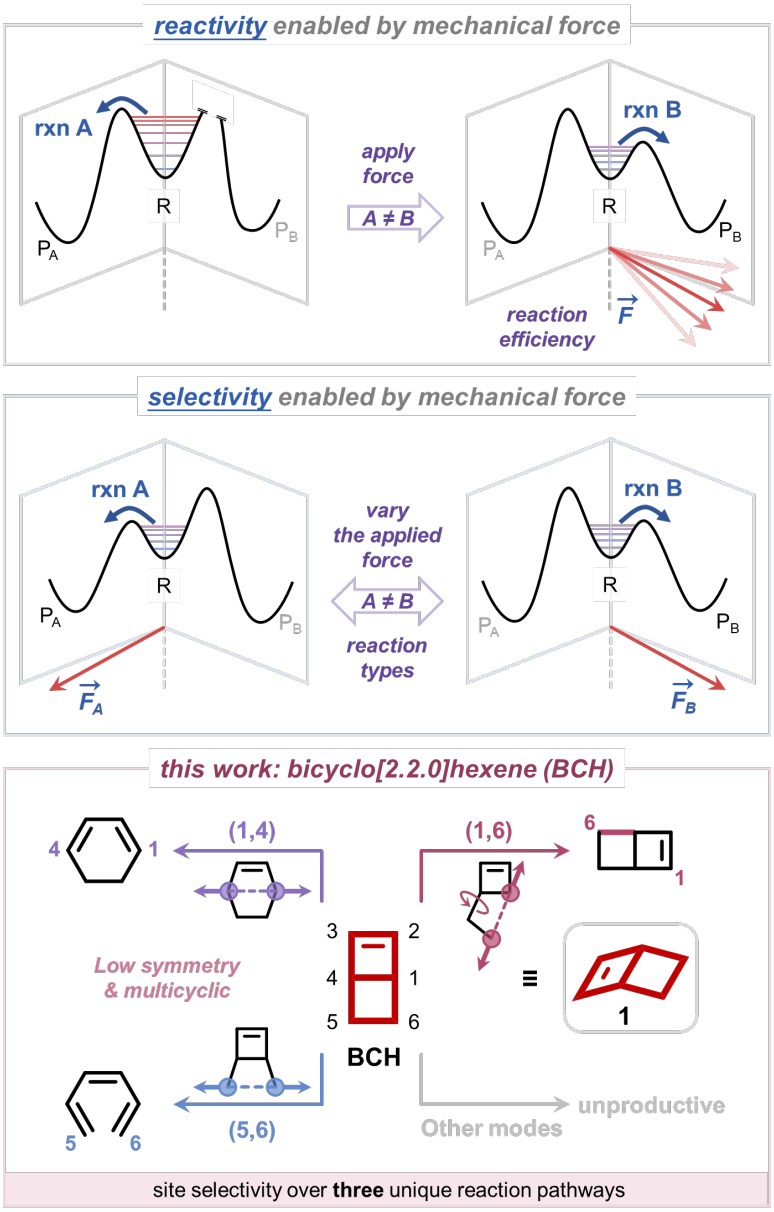

Figure 1. Force-governed chemoselectivity via multi-modal activation of bicyclo[2.2.0]hexene (BCH) mechanophore. Numberings on the products follow the inactivated BCH to help show structural relationship before and after reaction.

One strategy to change the ways of force exertion on a mechanophore is to design and test different regioisomers, as the relative position between pulling points affects the alignment between the applied force and the targeted bond. Benefited from the synthetic modularity, a variety

of regioisomers of mechanophores have been tested, such as spiropyran,[36-40] naphthopyran,[41] oxazine,[42] furan-maleimide adduct,[43,44] anthracene-maleimide adduct,[45] cyclobutane,[46,47] cubane,[48] and carborane.[49] In some cases, only one specific regioisomer was found to be mechanochemically active[48,49] and in rare cases, regioisomerism did not show impact on reactivity.[28,45] Another strategy to influence the coupling of force is to use stereoisomers of mechanophores, as the stereochemical relationship between pulling handles also controls the effectiveness of applied force.[50,51] By leveraging the stereochemistry during the construction of strained cycles, a wide range of four-membered[8,35,52-54] and three-membered rings,[9,11,54-56] and adduct from Diels-Alder reaction[43,44] have been examined. Other unique scenarios find use of flex modes[14,57-60] rather than tension modes to induce scission of bonds that are connected to the bended center but not necessarily strained. Overall, these existing examples showed that mechanochemical reactivity is highly sensitive and dependent on the applied force. Therefore, changing the ways in which force is exerted on one mechanophore, in principle, has the potential to lead to different mechanochemical reactivity (i.e., chemoselectivity) from that single mechanophore.

We envisioned that a multicyclic mechanophore with a low symmetry will be ideal to demonstrate how reactivity depends on the directionality of the exerted force. Such a mechanophore should feature multiple distinctive bonds and, at the same time, be synthetically accessible. Bicyclo[2.2.0]hexene (**BCH**) caught our attention as a candidate mechanophore for its structural simplicity, multicyclic skeleton, and a relatively low molecular symmetry (Figure 1, bottom box). BCH belongs to a family of ladderane- or ladderene-like molecules, which have been found as a dominant lipid in anaerobic bacteria central in the oceanic nitrogen cycle[61,62] and hence attracted increasing attention towards their synthesis.[63-65] The development of ladderane synthesis further expands the applications of this family of compounds in the area of organic synthesis,[66-68]

medicinal chemistry as bioisoteres,[69] and materials sciences.[70,71] The ladderane family has also been repurposed in polymer mechanochemistry quite successfully by Xia as an emergent mechanophore,[72,73] demonstrating insulator-to-semiconductor transformation,[74] cascade mode of activation,[34] and the ability to access otherwise inaccessible fluorinated polyacetylene.[75]

RESULTS AND DISCUSSION

Design and Synthesis of Multimodal BCH Mechanophores. We computationally screened nine possible activation modes of BCH by stretching the mechanophore on different combinations of pulling points. The in-silico molecular extension was performed by the constrained geometries simulate external force (CoGEF) analysis[76] on the *cis*-isomers (if present) for their expected higher mechanochemical activity,[35,52,53] and with carboxylate group as the pulling handle (Figure S2). Activation modes with scission on the linker or with a rupture force exceeding that of a typical C–C bond,[77] i.e., ~6 nN, were considered unproductive, yielding three chemically distinctive activation modes (Figure 1, bottom box). The 1,4-activation mode is an anti-Woodward–Hoffmann, 4π-electrocyclic ring-opening reaction[8,51] on the cyclobutene fragment, cleaving the weakest bond of BCH on the thermal energy landscape. The 5,6-activation mode is a stepwise retro-[2+2] cycloreversion reaction on the cyclobutane fragment.[26,35,46,74] The 1,6-activation mode generates a diradical intermediate followed by the formation of a new C–C bond. This formal completion of a 1,3-rearrangement reaction is particularly intriguing as it turns a force-responsive 1,6-BCH into a force-resistant 2,5-BCH, equivalent to a mechanochemical energy sink. Overall, the mutually distinctive product profile exhibited by different reaction paths ensures a simplified and definitive assignment on the identity of the activated bond when respective BCH isomers were put under mechanical stress.

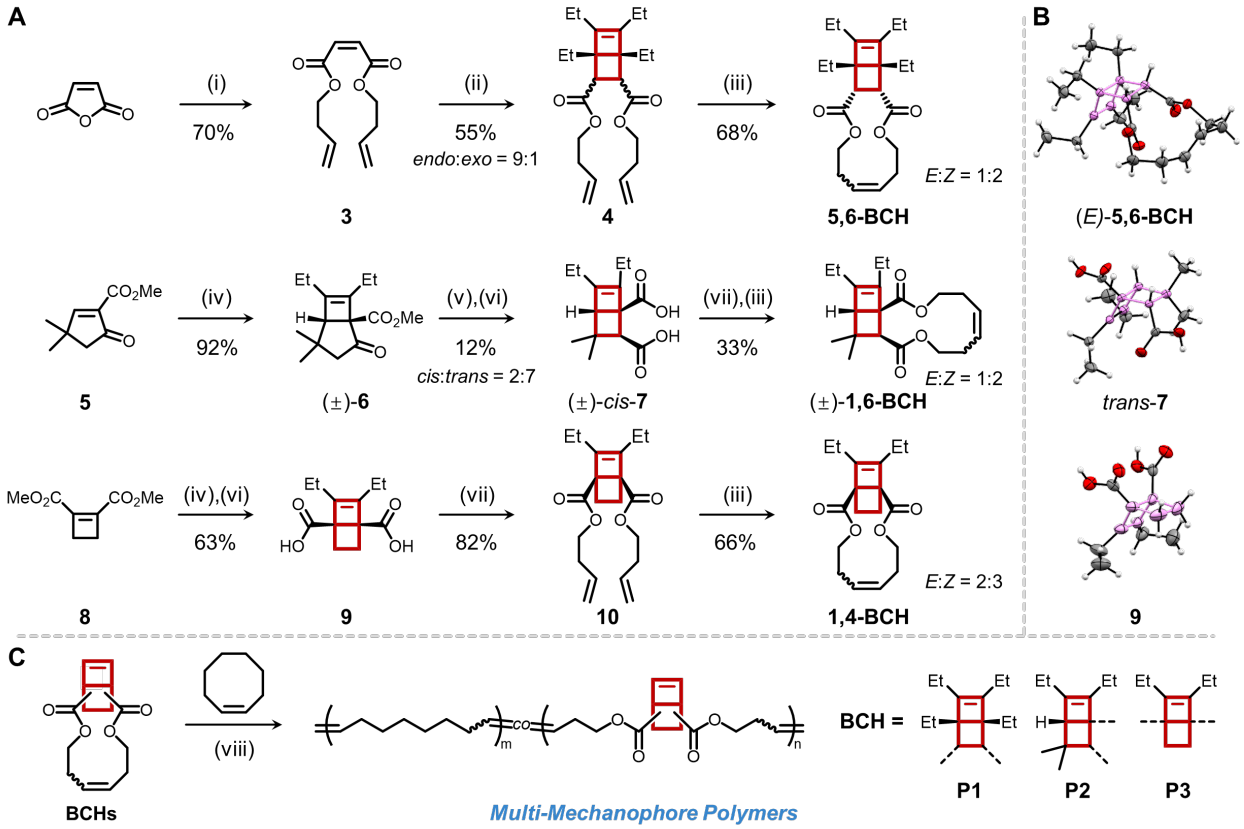

Figure 2. Preparation of polymers containing in-chain BCHs. (A) Synthesis of (A) BCH comonomers. (B) Crystal structures of key intermediate. (C) Polymer synthesis via ROMP. Conditions: (i) 3-butene-1-ol, $KHSO_4$, PhMe, 150 °C. (ii) 3-hexyne, $AlCl_3$, CH_2Cl_2, –15 °C; then DMSO, –15 °C. (iii) Grubbs' catalyst II, CH_2Cl_2, reflux. (iv) 3-hexyne, thioxanthone, 365 nm, CH_2Cl_2, rt. (v) 4-AcNHPhSO$_2$N$_3$, DBU, MeCN, rt; then MeOH, 365 nm, rt. (vi) KOH, MeOH/H_2O, rt. (vii) 3-butene-1-ol, EDCI, DMAP, CH_2Cl_2 or THF, rt. (viii) Grubbs' catalyst II, $CHCl_3$, *cis*-4-octene, reflux (or without *cis*-4-octene in CH_2Cl_2, rt). Color code in (B): carbon, grey; oxygen; red; hydrogen, white; BCH backbone, pink. All thermal ellipsoids are shown at 50% probability.

The BCH backbone with different substitution patterns was approached via cycloaddition strategies that utilize strained, cyclic alkene substrates (Figure 2A). The 5,6-BCH backbone was constructed via Diels–Alder [4+2] cycloaddition reaction between the electron-poor maleate **3** and

cyclobutadiene that was gradually released from its $AlCl_3$ complex.[78] The 1,6-BCH backbone was first introduced as a 4/5 ring system (**6**) by an energy-transfer [2+2] cycloaddition[69,79] between 3-hexyne and a cyclopentene-based unsaturated ester **5**, followed by a Wolff rearrangement that led to ring contraction to afford the 4/4 backbone (**7**). The *cis*-isomer was isolated for monomer preparation. The 1,4-BCH backbone was also built by an energy-transfer [2+2] reaction but using a cyclobutene dicarboxylate **8** to directly access the 4/4 ring system (**9**). Terminal alkenes were introduced to BCHs by esterification, and ring-closing metathesis was carried out to form macrocyclic monomers of BCHs for ring-opening metathesis polymerization (ROMP).

The stereochemistry of BCHs was confirmed by X-ray crystal structure analysis on the macrocyclic monomer or the key intermediates (Figure 2B). The *E*-isomer of **5,6-BCH** crystalized out from the *E*,*Z* mixture, allowing us to confirm the *endo* stereochemistry of the 5,6-substituted mechanophore. The *cis*-isomer of **1,6-BCH** was a minor product from Wolff rearrangement reaction, hence the *trans*-isomer was used for its availability to indirectly confirm the stereochemistry of **1,6-BCH**. Finally, the stereochemistry of **1,4-BCH** was confirmed using the readily crystalline diacid intermediate **9** and no isomerization is expected in subsequent steps due to the lack of acidic α-protons. Polymerization of BCHs with *cis*-cyclooctene comonomer (Figure 2C) via ROMP rendered linear copolymers **P1**–**P3**, containing multiple in-chain BCH mechanophores (35–50 mol%).[15] NMR spectra before and after polymerization showed retention of the BCH structures and their stereochemistry in the polymers (Figures S23–S25).

Mechanochemical Activation of BCHs. We performed mechanochemical activation of BCHs via solution sonication of polymers. We first looked at the activation of 5,6-BCH in polymer **P1**. The ^{1}H NMR spectrum of the polymer after sonication features multiple new alkene methine CH peaks at δ = 5.6 ppm (Figure 3A, blue) and diminishing methine peaks on the BCH

at δ = 3.2 ppm (Figure 3A, green), suggesting the cyclobutane fragment in 5,6-BCH has been activated into alkenes, nominally, trienes. The triene backbone was successfully mapped out by the ^{1}H-^{13}C heteronuclear multiple-bond correlation (HMBC) spectrum (Figures S30–S32). The triene formation was further corroborated by the linear relationship between increasing long-wavelength UV absorption and BCH conversion monitored by ^{1}H-NMR (Figure S33). The stereochemistry of the triene products was resolved by the ^{1}H NMR spectra of small-molecule references (Figure S34) and verified by the spatial proximity of alkene CH protons with ethyl substituents (Figures S35 and S36): the two flanking double bonds were found to exist in *E*,*Z*-, *E*,*E*-, and *Z*,*Z*-stereoisomers with a ratio of 2.6:1.0:0.2, and isomerization of the central double bond was not observed.[80] In sum, the retro-[2+2] cycloreversion reaction of BCH into trienes was successfully achieved by applying external forces across the C5–C6 bond.

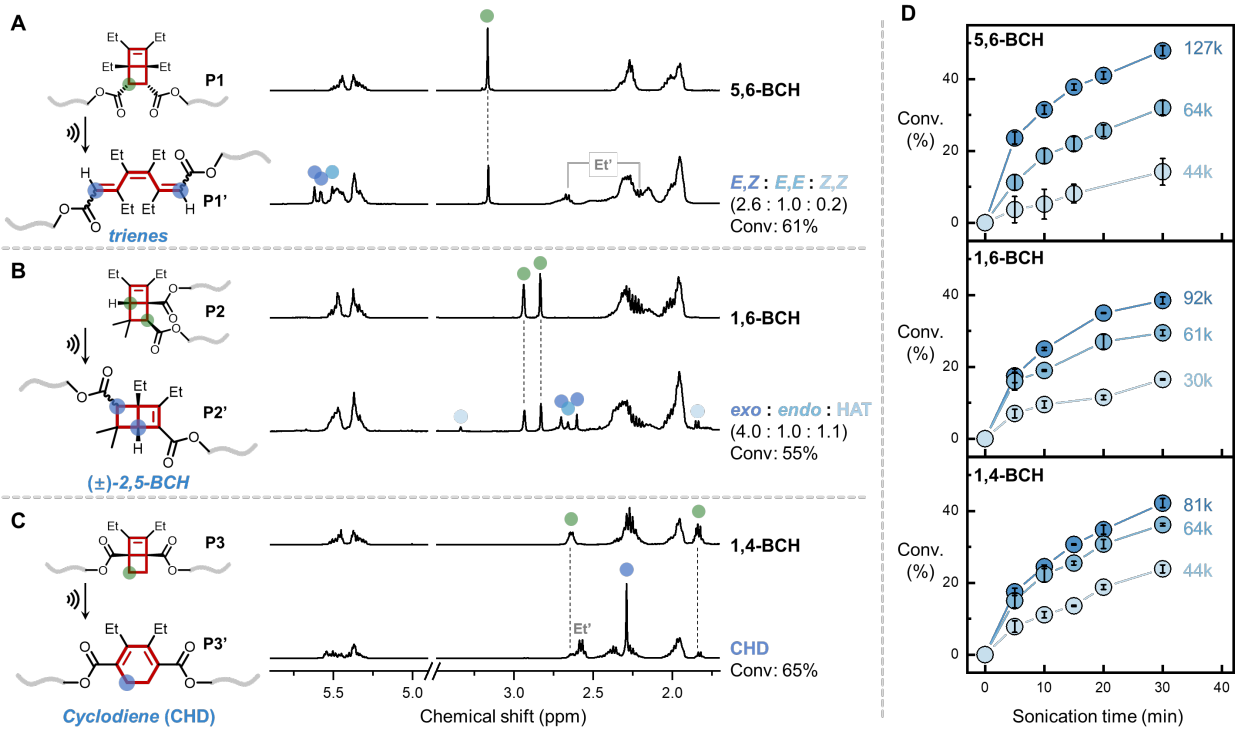

Figure 3. Mechanochemical activation of BCHs. Stacked ^{1}H NMR spectra of polymers containing in-chain (A) **5,6-BCH**, (B) **1,6-BCH**, and (C) **1,4-BCH** before and after sonication (100–130 kDa,

20 kHz, 9.4 W/cm^2, –10 ºC, THF, 2–2.5 h on time). Characteristic ^{1}H peaks of reactants and products are highlighted. The listed products are named after the variable stereochemistry, as indicated by wavy bonds. HAT represents a side product arose from 1,5-hydrogen atom transfer. (D) Rate of mechanochemical conversion for BCHs in polymers of varying molecular weights.

We then sonicated polymer **P2** containing in-chain 1,6-BCH (Figure 3B), which is expected to undergo a 1,3-migration reaction. Upon activation, characteristic methine CH proton resonances of 1,6-BCH backbone at δ = 2.8 and 2.9 ppm (Figure 3B, green) were observed to decrease while a new set of methine protons emerged at around 2.7 ppm (Figure 3B, blue; Figure S39). HMBC analysis disclosed three sets of product resonance peaks, two of which shared resembling connectivity (Figures S44 and S45) that are consistent with being a pair of 2,5-BCH stereoisomers. The stereochemistry of the C5-carboxylate in 2,5-BCH was determined by the spatial proximity of its α-proton with the bridge-head CH proton on the *exo*-face, yielding an *exo*:*endo* ratio of 4:1. The third product was represented by the singlet at δ = 3.3 ppm (Figure 3B, light blue), and other hidden peaks uncovered by ^{1}H-^{13}C HMBC analysis (Figure S46). We resorted to metadynamics sampling[81] on the force-modified potential surface using DFT to assist in product identification. In addition to confirm the formation of 2,5-BCHs, the simulations revealed a 1,5-hydrogen atom transfer (HAT) reaction[82-84] from one of the ethyl groups to the mechanochemically formed diradical (Table S6), leading to a side product whose resonance peaks agree with the third species observed (Figure S46). The presence of HAT side product and the 2,5-BCH stereoisomers suggests that the rearrangement reaction follows a stepwise mechanism. The C6 radical, formed upon C1–C6 scission in 1,6-BCH, undergoes radical recombination with the C3 carbon, which carries a radical character via through-bond resonance with the C1 radical. An alternative mechanism uncovered by the simulations involved further scission to form

cyclobutadiene (Table S6, entry 2), which can undergo Diels–Alder [4+2] cycloaddition with the pairing alkene to reform BCHs. This mechanism was ruled out, however, since cyclobutadiene would have unbiasedly involved any alkene in the polymer to form new BCHs that we did not observe.

We next investigated the mechanochemical activation of 1,4-BCH in polymer **P3**. The ^{1}H NMR spectrum of polymer upon sonication shows decreased intensity of cyclobutane methylene CH_2 peaks at δ = 2.7 and 1.8 ppm for *exo*- and *endo*-orientations, respectively (Figure 3C, green). Concomitantly, a single, merged methylene peak appeared at δ = 2.3 ppm (Figure 3C, blue), indicative of a more flexible backbone than a cyclobutane. The formation of cyclohexadiene was confirmed using the ^{1}H and ^{13}C NMR spectra of a small molecule reference (Figure S48) in conjunction with the ^{1}H-^{13}C HMBC spectrum (Figure S50). Our observation is consistent with the predicted 4π-electrocyclic ring-opening reaction when mechanical stress is exerted along the C1–C4 direction of BCH. The *E*,*E*-isomer of diene was validated by X-ray crystal structure of the reference compound, implying that the mechanochemical activation follows a disrotatory path.[8,85]

Validating Force-Driven Chemoselectivity. To examine the potential contribution of heat in sonication-induced mechanochemical activation, we prepared polymers using cyclooctenes with side-chain BCHs. Since side chains are not pulled on two opposite directions, no force but only heat (if any) is applied to the polymer. After 2 h of sonication, no conversion was observed for side-chain BCHs (Figures S51–S53). Even the 1,4-BCH, whose thermal instability necessitated a room temperature ROMP condition, remained intact, confirming that thermally induced activation is insignificant during sonication. We further prepared a series of polymers containing in-chain BCHs with varied molecular masses. Faster mechanochemical

conversion was observed when polymers of higher molecular masses were sonicated (Figure 3D), evincing force-driven reactivity[52,86] for the observed transformations of different BCH isomers.

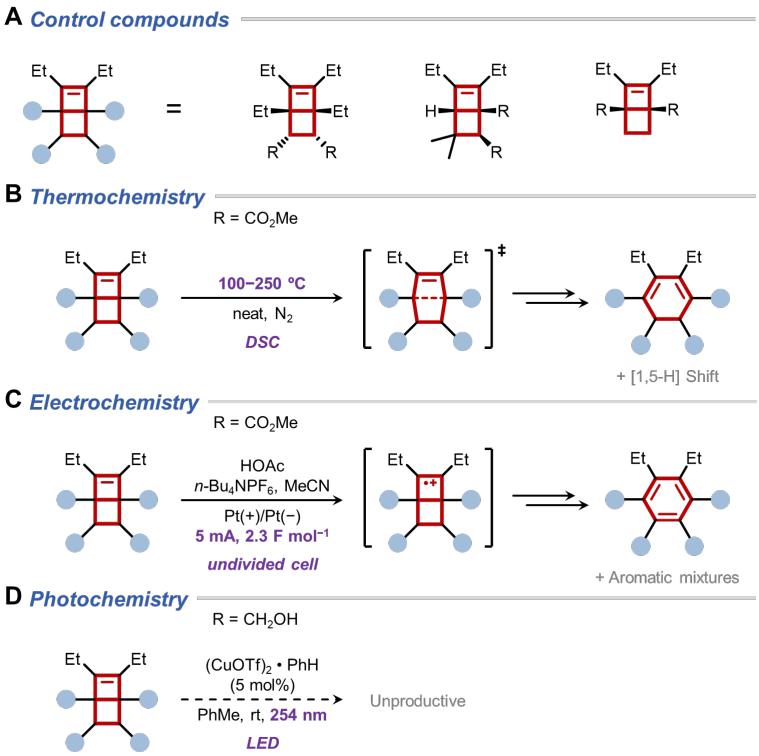

Figure 4. Chemoselectivity of (A) small-molecule control BCHs under (B) thermal, (C) electrochemical, and (D) photochemical treatments. DSC: differential scanning calorimetry.

To confirm that the observed chemoselectivity of BCH is unique under mechanochemical conditions, we ran control reactions on carboxylates or hydroxyl-derivatives of BCH isomers under thermal, electrochemical, and photochemical conditions (Figure 4). Upon heating, all three BCH isomers underwent thermal ring-opening reactions via scission of C1–C4 bonds, as the measured reaction barriers are consistent with those computationally predicted for the 1,4-scission of each BCH (Figure S72). The electrochemical reactive sites of BCH isomers, revealed by cyclic voltammetry and constant-current electrolysis, were found to be the electron-rich double bonds irrespective of the substitution pattern (Figure S77). The photochemical attempts were not

successful, probably due to steric hindrance, as unsubstituted BCH has been shown to undergo ring-opening or dimerization under light.[64] Nonetheless, the similar UV-vis spectra (Figure S78) and orbital contributions to the first singlet excited states (Figure S79) suggests that the photochemical reactivity of BCHs, if accessed, would have been similar across isomers. Overall, we showed that although regioisomers of BCH displayed variable mechanochemical selectivity, the preferred reactivity of regioisomers under heat and other stimuli remains unvaried.

Theoretical Analysis of Bond-Specific Activation. We analyzed the force-modified minimum-energy paths (FMMEP) of the unsubstituted BCH core to see if the changes in substitution altered the potential energy landscape of the parent BCH. The barriers of bond scission reactions for C5–C6, C1–C6, and C1–C4 bonds were calculated in each mechanochemical scenario under 0.0 to 3.0 nN external forces (Figure 5B, solid circles). In each scenario, only the best aligned C–C bond displays a noticeable force-enhanced reactivity, reflected by the negative slopes in barrier-force curves in Figure 5B, reaching a low enough barrier for kinetically competent scission reaction (<17 kcal/mol).[33,51] That is, only C5–C6 bond is reactive in the 5,6-alignment; the same goes for C1–C6 and C1–C4, showing that the unsubstituted BCHs display the same reactive bonds as the substituted ones. Furthermore, at any given force, the modified scission barriers of the three reactive bonds follow the order of C5–C6 > C1–C6 > C1–C4 by comparing the three traces of solid circles with negative slopes across Figure 5B. Thus, the scission reactivity of C–C bonds is expected to follow the opposite: C1–C4 > C1–C6 > C5–C6. This theoretical prediction based on unsubstituted BCH conforms with the experimental kinetics of carboxylate-substituted BCHs (Figure S66),[86,87] suggesting the substitution does not change the relative reactivity between different isomers either. Further FMMEP analysis with the carboxylate-substituted BCHs showed barrier-force curves closely tracing those of the unsubstituted ones

(Figure 5B, downward traces with solid vs. open circles) above 0.5 nN, confirming the innocence of substitution in reshaping the reactivity landscape of BCH. Deviations were seen in the low-force regimes of substituted BCHs, possibly due to the attractive dipolar interactions between carbonyl linkers. But at this point the barriers are too high (>30 kcal/mol) for kinetically competent mechanochemical activation, leaving the deviations inconsequential in affecting reactivity.

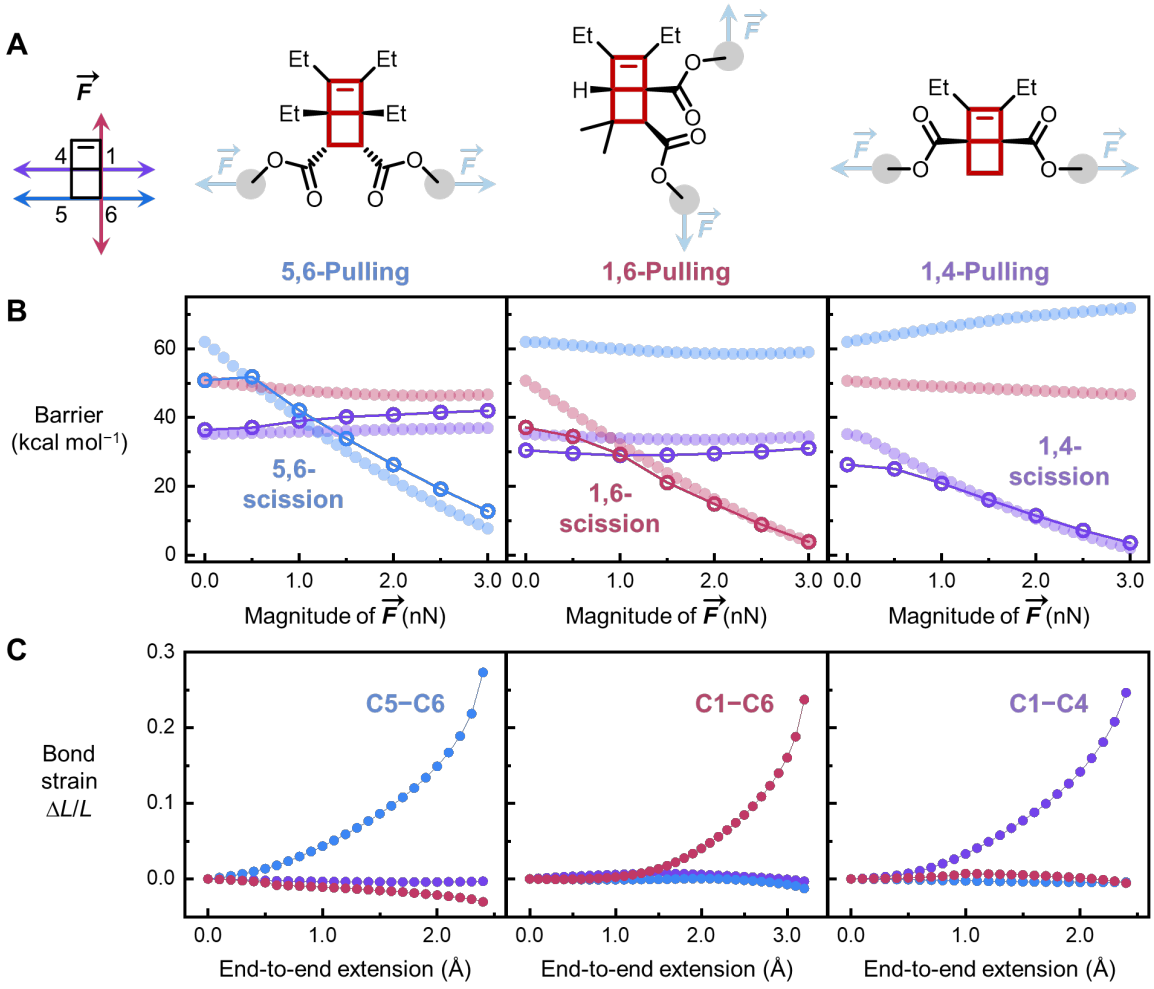

Figure 5. Force-modified reaction barriers of BCHs. (A) Three pulling scenarios are shown using carboxylate-substituted model compounds (**BCH-Me**). (B) Scission barriers of C5–C6, C1–C6, and C1–C4 bonds as a function of force in the unsubstituted BCH under each activation scenario (solid circles). Scission barriers of the mechanochemically activated bonds in each scenario are

also shown along with the thermally preferred 1,4-scission for **BCH-Me**'s (empty circles). (C) Strain of C5–C6, C1–C6, and C1–C4 bonds by CoGEF analysis in different pulling scenarios. Color codes: 5,6-scission, blue; 1,6-scission, red; 1,4-scission, purple.

The chemoselectivity of BCH activation is further attested by theoretical analysis. In all activation modes, only the C–C bonds along the pulling directions were found to be selectively modified; their scission barriers decline (Figure 5B) and their bond lengths elongate (Figure 5C) under force. Regarding the molecular geometry, the reactive C–C bonds are either parallel (e.g., C5–C6 and C1–C4) or perpendicular (e.g., C1–C6 and C1–C4) to each other, allowing selective exertion of mechanical work to the respective bonds. From the energy point of view, the mechanical work needs to overcome the stability differences between the extended C–C bond and the thermally preferred C–C bond in order to trigger the observed scission reaction. In 1,4-BCH, the mechanical work is applied to the thermally labile C1–C4 bond, resulting in a highly active mechanochemical reaction. In other scenarios, the 1,4-scission is competitive. Therefore, we observed that there is a minimum exertion of work required to enable bond-specific transformations: the cross-over regime is ~1.0 nN for both 5,6- and 1,6-scission modes to be in favor over 1,4-scission (Figure 5B), at which point the barriers remain kinetically prohibitive, allowing BCH to display high chemoselectivity across all effective range of forces.

The experimentally derived diradical intermediates and mechanochemical products were further confirmed by theoretical analyses, including molecular dynamics. The formation of diradical intermediates in the 5,6- and 1,6-activtion were found on the force-modified reaction paths. While the 5,6-scission intermediate becomes kinetically unstable under higher force due to the reduced barrier of the second scission (Table S13), the kinetic stability of 1,6-scission

intermediate increases with higher stress (Table S17). *Ab-initio* steered molecular dynamics simulations were then performed on model compounds **BCH-Me**'s with a 1.0-nN force to evaluate product composition. Consistent with experimental findings, the simulations showed that 5,6-BCH leads to trienes with flanking double bonds exist in mixed *E*/*Z* forms, 1,6-BCH primarily forms *exo*-2,5-BCH with HAT side product, and 1,4-BCH yields cyclohexadiene (Table S19).

CONCLUSION

In conclusion, we have shown that the BCH mechanophore features multiple activation modes. By using different regioisomers, the mechanical force is applied across distinctive C–C bonds to trigger unique reaction pathways. In the case of BCH, retro-[2+2] cycloreversion, 1,3-allylic migration, and 4π-electrocyclic ring-opening reactions are accessed using the same mechanophore. Conventionally, either reaction efficiency or product distribution from the same rate-determining step has been successfully controlled by external forces. The discovery of the BCH mechanophore highlights an emergent possibility to access chemoselectivity between reactions of dissimilar mechanisms. In alliance with other chemical or physical approaches, it is possible to define and target uncommon reactive sites for bond-specific chemical transformations using polymer mechanochemistry.

ASSOCIATED CONTENT

Supporting Information

Experimental and computational procedures, synthesis and characterization of new compounds, GPC and NMR data for polymers, 2D NMR for product assignments, NMR data for kinetics and control studies, and computational results (PDF)

Cartesian coordinates of all computed compounds (ZIP)

AUTHOR INFORMATION

Corresponding Author

Jan Meisner − *Institute for Physical Chemistry, Faculty of Mathematics and Natural Sciences, Heinrich Heine University Düsseldorf, Düsseldorf, 40225, Germany*; ORCID: 0000-0002-1301-2612; Email: meisner@hhu.de

Rong Zhu − *Beijing National Laboratory for Molecular Sciences, Key Laboratory of Bioorganic Chemistry and Molecular Engineering of Ministry of Education, and College of Chemistry and Molecular Engineering, Peking University, Beijing, 100871, China*; ORCID: 0000-0001-5035-3531; Email: rongzhu@pku.edu.cn

Yun Liu − *Beijing National Laboratory for Molecular Sciences, Center for Soft Matter Science and Engineering, Key Laboratory of Polymer Chemistry and Physics of Ministry of Education, College of Chemistry and Molecular Engineering, Peking University, Beijing 100871, China*; ORCID: 0000-0001-7077-363X; Email: yun.liu@pku.edu.cn

Authors

Shihao Ding − *Beijing National Laboratory for Molecular Sciences, Center for Soft Matter Science and Engineering, Key Laboratory of Polymer Chemistry and Physics of Ministry*

of Education, College of Chemistry and Molecular Engineering, Peking University, Beijing 100871, China

Wenkai Wang − *Beijing National Laboratory for Molecular Sciences, Key Laboratory of Bioorganic Chemistry and Molecular Engineering of Ministry of Education, and College of Chemistry and Molecular Engineering, Peking University, Beijing, 100871, China*

Anne Germann − *Institute for Physical Chemistry, Faculty of Mathematics and Natural Sciences, Heinrich Heine University Düsseldorf, Düsseldorf, Germany*; ORCID: 0000-0003-1429-9659

Yiting Wei − *Beijing National Laboratory for Molecular Sciences, Center for Soft Matter Science and Engineering, Key Laboratory of Polymer Chemistry and Physics of Ministry of Education, College of Chemistry and Molecular Engineering, Peking University, Beijing 100871, China*

Tianyi Du − *Beijing National Laboratory for Molecular Sciences, Center for Soft Matter Science and Engineering, Key Laboratory of Polymer Chemistry and Physics of Ministry of Education, College of Chemistry and Molecular Engineering, Peking University, Beijing 100871, China*

Author Contributions

‡These authors contributed equally.

Notes

The authors declare no competing financial interest.

ACKNOWLEDGMENTS

This work was supported by the startup funds from College of Chemistry and Molecular Engineering at Peking University and Beijing National Laboratory for Molecular Sciences. W.W. and R.Z. acknowledge the financial support from the Natural Science Foundation of China (22171012 and 22222101). A.G. and J.M. acknowledge the support of computational infrastructure provided by the Centre for Information and Media Technology at Heinrich-Heine University Düsseldorf. We thank Beijing NMR Center at Peking University and Dr. Hongwei Li for their assistance in 2D NMR experiments, and W. Zhong for absorption spectra acquisition. T.D. thanks High-performance Computing Platform of Peking University for provision of computational resource. J.M. is grateful for a materials cost allowance from the Fonds der Chemischen Industrie.

REFERENCES

(1) Sinha, A.; Hsiao, M. C.; Crim, F. F. Controlling bimolecular reactions: Mode and bond selected reaction of water with hydrogen atoms. *J. Chem. Phys.* **1991**, *94*, 4928–4935.
(2) Zare, R. N. Laser control of chemical reactions. *Science* **1998**, *279*, 1875–1879.
(3) Thomas, A.; Lethuillier-Karl, L.; Nagarajan, K.; Vergauwe, R. M. A.; George, J.; Chervy, T.; Shalabney, A.; Devaux, E.; Genet, C.; Moran, J.; Ebbesen, T. W. Tilting a ground-state reactivity landscape by vibrational strong coupling. *Science* **2019**, *363*, 615–619.
(4) Yan, S.; Wu, Y. T.; Zhang, B.; Yue, X. F.; Liu, K. Do vibrational excitations of CHD_3 preferentially promote reactivity toward the chlorine atom? *Science* **2007**, *316*, 1723–1726.
(5) Killelea, D. R.; Campbell, V. L.; Shuman, N. S.; Utz, A. L. Bond-selective control of a heterogeneously catalyzed reaction. *Science* **2008**, *319*, 790–793.
(6) Sau, A.; Nagarajan, K.; Patrahau, B.; Lethuillier-Karl, L.; Vergauwe, R. M. A.; Thomas, A.; Moran, J.; Genet, C.; Ebbesen, T. W. Modifying Woodward–Hoffmann stereoselectivity under vibrational strong coupling. *Angew. Chem., Int. Ed.* **2021**, *60*, 5712–5717.
(7) Zhang, W.; Kawamata, H.; Liu, K. CH stretching excitation in the early barrier F + CHD_3 reaction inhibits CH bond cleavage. *Science* **2009**, *325*, 303–306.
(8) Hickenboth, C. R.; Moore, J. S.; White, S. R.; Sottos, N. R.; Baudry, J.; Wilson, S. R. Biasing reaction pathways with mechanical force. *Nature* **2007**, *446*, 423–427.
(9) Lenhardt, J. M.; Ong, M. T.; Choe, R.; Evenhuis, C. R.; Martinez, T. J.; Craig, S. L. Trapping a diradical transition state by mechanochemical polymer extension. *Science* **2010**, *329*, 1057–1060.
(10) Huang, W.; Wu, X.; Gao, X.; Yu, Y.; Lei, H.; Zhu, Z.; Shi, Y.; Chen, Y.; Qin, M.; Wang, W.; Cao, Y. Maleimide–thiol adducts stabilized through stretching. *Nat. Chem.* **2019**, *11*, 310–319.
(11) Jung, S.; Yoon, H. J. Mechanical force induces ylide-free cycloaddition of nonscissible aziridines. *Angew. Chem., Int. Ed.* **2020**, *59*, 4883–4887.
(12) Nixon, R.; De Bo, G. Three concomitant C–C dissociation pathways during the mechanical activation of an N-heterocyclic carbene precursor. *Nat. Chem.* **2020**, *12*, 826–831.
(13) Evans, E. Probing the relation between force–lifetime–and chemistry in single molecular bonds. *Annu. Rev. Biophys. Biomol. Struct.* **2001**, *30*, 105–128.
(14) Akbulatov, S.; Tian, Y.; Huang, Z.; Kucharski, T. J.; Yang, Q.; Boulatov, R. Experimentally realized mechanochemistry distinct from force-accelerated scission of loaded bonds. *Science* **2017**, *357*, 299–303.
(15) Lee, B.; Niu, Z.; Wang, J.; Slebodnick, C.; Craig, S. L. Relative mechanical strengths of weak bonds in sonochemical polymer mechanochemistry. *J. Am. Chem. Soc.* **2015**, *137*, 10826–10832.
(16) Wu, M.; Li, Y.; Yuan, W.; De Bo, G.; Cao, Y.; Chen, Y. Cooperative and geometry-dependent mechanochromic reactivity through aromatic fusion of two rhodamines in polymers. *J. Am. Chem. Soc.* **2022**, *144*, 17120–17128.
(17) He, W.; Yuan, Y.; Wu, M.; Li, X.; Shen, Y.; Qu, Z.; Chen, Y. Multicolor chromism from a single chromophore through synergistic coupling of mechanochromic and photochromic subunits. *Angew. Chem., Int. Ed.* **2023**, e202218785.
(18) Potisek, S. L.; Davis, D. A.; Sottos, N. R.; White, S. R.; Moore, J. S. Mechanophore-linked addition polymers. *J. Am. Chem. Soc.* **2007**, *129*, 13808–13809.

(19) Li, J.; Nagamani, C.; Moore, J. S. Polymer mechanochemistry: from destructive to productive. *Acc. Chem. Res* **2015**, *48*, 2181–2190.
(20) Piermattei, A.; Karthikeyan, S.; Sijbesma, R. P. Activating catalysts with mechanical force. *Nat. Chem.* **2009**, *1*, 133–137.
(21) Wang, J.; Kouznetsova, T. B.; Boulatov, R.; Craig, S. L. Mechanical gating of a mechanochemical reaction cascade. *Nat. Commun.* **2016**, *7*, 13433.
(22) Hu, X.; McFadden, M. E.; Barber, R. W.; Robb, M. J. Mechanochemical regulation of a photochemical reaction. *J. Am. Chem. Soc.* **2018**, *140*, 14073–14077.
(23) McFadden, M. E.; Robb, M. J. Force-dependent multicolor mechanochromism from a single mechanophore. *J. Am. Chem. Soc.* **2019**, *141*, 11388–11392.
(24) Kosuge, T.; Zhu, X.; Lau, V. M.; Aoki, D.; Martinez, T. J.; Moore, J. S.; Otsuka, H. Multicolor mechanochromism of a polymer/silica composite with dual distinct mechanophores. *J. Am. Chem. Soc.* **2019**, *141*, 1898–1902.
(25) Hu, X.; Zeng, T.; Husic, C. C.; Robb, M. J. Mechanically triggered small molecule release from a masked furfuryl carbonate. *J. Am. Chem. Soc.* **2019**, *141*, 15018–15023.
(26) Hsu, T. G.; Zhou, J.; Su, H.; Schrage, B. R.; Ziegler, C. J.; Wang, J. A polymer with "locked" degradability: superior backbone stability and accessible degradability enabled by mechanophore installation. *J. Am. Chem. Soc.* **2020**, *142*, 2100–2104.
(27) Lin, Y.; Kouznetsova, T. B.; Craig, S. L. Mechanically gated degradable polymers. *J. Am. Chem. Soc.* **2020**, *142*, 2105–2109.
(28) Lu, Y.; Sugita, H.; Mikami, K.; Aoki, D.; Otsuka, H. Mechanochemical reactions of bis(9-methylphenyl-9-fluorenyl) peroxides and their applications in cross-linked polymers. *J. Am. Chem. Soc.* **2021**, *143*, 17744–17750.
(29) Overholts, A. C.; Razo, W. G.; Robb, M. J. Mechanically gated formation of donor-acceptor Stenhouse adducts enabling mechanochemical multicolour soft lithography. *Nat. Chem.* **2023**, *15*, 332–338.
(30) Hsu, T. G.; Liu, S.; Guan, X.; Yoon, S.; Zhou, J.; Chen, W. Y.; Gaire, S.; Seylar, J.; Chen, H.; Wang, Z.; Rivera, J.; Wu, L.; Ziegler, C. J.; McKenzie, R.; Wang, J. Mechanochemically accessing a challenging-to-synthesize depolymerizable polymer. *Nat. Commun.* **2023**, *14*, 225.
(31) Tian, Y.; Cao, X.; Li, X.; Zhang, H.; Sun, C. L.; Xu, Y.; Weng, W.; Zhang, W.; Boulatov, R. A polymer with mechanochemically active hidden length. *J. Am. Chem. Soc.* **2020**, *142*, 18687–18697.
(32) Wang, Z.; Zheng, X.; Ouchi, T.; Kouznetsova, T. B.; Beech, H. K.; Av-Ron, S.; Matsuda, T.; Bowser, B. H.; Wang, S.; Johnson, J. A.; Kalow, J. A.; Olsen, B. D.; Gong, J. P.; Rubinstein, M.; Craig, S. L. Toughening hydrogels through force-triggered chemical reactions that lengthen polymer strands. *Science* **2021**, *374*, 193–196.
(33) Bowser, B. H.; Wang, S.; Kouznetsova, T. B.; Beech, H. K.; Olsen, B. D.; Rubinstein, M.; Craig, S. L. Single-event spectroscopy and unravelling kinetics of covalent domains based on cyclobutane mechanophores. *J. Am. Chem. Soc.* **2021**, *143*, 5269–5276.
(34) Chen, Z.; Zhu, X.; Yang, J.; Mercer, J. A. M.; Burns, N. Z.; Martinez, T. J.; Xia, Y. The cascade unzipping of ladderane reveals dynamic effects in mechanochemistry. *Nat. Chem.* **2020**, *12*, 302–309.
(35) Liu, Y.; Holm, S.; Meisner, J.; Jia, Y.; Wu, Q.; Woods, T. J.; Martinez, T. J.; Moore, J. S. Flyby reaction trajectories: Chemical dynamics under extrinsic force. *Science* **2021**, *373*, 208–212.

(36) Davis, D. A.; Hamilton, A.; Yang, J.; Cremar, L. D.; Van Gough, D.; Potisek, S. L.; Ong, M. T.; Braun, P. V.; Martínez, T. J.; White, S. R.; Moore, J. S.; Sottos, N. R. Force-induced activation of covalent bonds in mechanoresponsive polymeric materials. *Nature* **2009**, *459*, 68–72.
(37) Lee, C. K.; Diesendruck, C. E.; Lu, E.; Pickett, A. N.; May, P. A.; Moore, J. S.; Braun, P. V. Solvent swelling activation of a mechanophore in a polymer network. *Macromolecules* **2014**, *47*, 2690–2694.
(38) Gossweiler, G. R.; Kouznetsova, T. B.; Craig, S. L. Force-rate characterization of two spiropyran-based molecular force probes. *J. Am. Chem. Soc.* **2015**, *137*, 6148–6151.
(39) Kim, T. A.; Robb, M. J.; Moore, J. S.; White, S. R.; Sottos, N. R. Mechanical reactivity of two different spiropyran mechanophores in polydimethylsiloxane. *Macromolecules* **2018**, *51*, 9177–9183.
(40) Lin, Y.; Barbee, M. H.; Chang, C. C.; Craig, S. L. Regiochemical effects on mechanophore activation in bulk materials. *J. Am. Chem. Soc.* **2018**, *140*, 15969–15975.
(41) Robb, M. J.; Kim, T. A.; Halmes, A. J.; White, S. R.; Sottos, N. R.; Moore, J. S. Regioisomer-specific mechanochromism of naphthopyran in polymeric materials. *J. Am. Chem. Soc.* **2016**, *138*, 12328–12331.
(42) Qian, H.; Purwanto, N. S.; Ivanoff, D. G.; Halmes, A. J.; Sottos, N. R.; Moore, J. S. Fast, reversible mechanochromism of regioisomeric oxazine mechanophores: Developing *in situ* responsive force probes for polymeric materials. *Chem* **2021**, *7*, 1080–1091.
(43) Stevenson, R.; De Bo, G. Controlling reactivity by geometry in retro-Diels−Alder reactions under tension. *J. Am. Chem. Soc.* **2017**, *139*, 16768–16771.
(44) Wang, Z.; Craig, S. L. Stereochemical effects on the mechanochemical scission of furan–maleimide Diels–Alder adducts. *Chem. Commun.* **2019**, *55*, 12263–12266.
(45) Baumann, C.; Willis-Fox, N.; Campagna, D.; Rognin, E.; Marten, P.; Daly, R.; Göstl, R. Regiochemical effects for the mechanochemical activation of 9-π-extended anthracene-maleimide Diels–Alder adducts. *J. Polym. Sci.* **2022**, *60*, 3128–3133.
(46) Zhang, H.; Li, X.; Lin, Y.; Gao, F.; Tang, Z.; Su, P.; Zhang, W.; Xu, Y.; Weng, W.; Boulatov, R. Multi-modal mechanophores based on cinnamate dimers. *Nat. Commun.* **2017**, *8*, 1147.
(47) Izak-Nau, E.; Campagna, D.; Baumann, C.; Göstl, R. Polymer mechanochemistry-enabled pericyclic reactions. *Polym. Chem.* **2020**, *11*, 2274–2299.
(48) Wang, L.; Zheng, X.; Kouznetsova, T. B.; Yen, T.; Ouchi, T.; Brown, C. L.; Craig, S. L. Mechanochemistry of cubane. *J. Am. Chem. Soc.* **2022**, *144*, 22865–22869.
(49) Sha, Y.; Zhou, Z.; Zhu, M.; Luo, Z.; Xu, E.; Li, X.; Yan, H. The mechanochemistry of carboranes. *Angew. Chem., Int. Ed.* **2022**, *61*, e202203169.
(50) Ong, M. T.; Leiding, J.; Tao, H.; Virshup, A. M.; Martínez, T. J. First principles dynamics and minimum energy pathways for mechanochemical ring opening of cyclobutene. *J. Am. Chem. Soc.* **2009**, *131*, 6377–6379.
(51) Brown, C. L.; Bowser, B. H.; Meisner, J.; Kouznetsova, T. B.; Seritan, S.; Martinez, T. J.; Craig, S. L. Substituent effects in mechanochemical allowed and forbidden cyclobutene ring-opening reactions. *J. Am. Chem. Soc.* **2021**, *143*, 3846–3855.
(52) Kryger, M. J.; Munaretto, A. M.; Moore, J. S. Structure–mechanochemical activity relationships for cyclobutane mechanophores. *J. Am. Chem. Soc.* **2011**, *133*, 18992–18998.
(53) Kean, Z. S.; Niu, Z.; Hewage, G. B.; Rheingold, A. L.; Craig, S. L. Stress-responsive polymers containing cyclobutane core mechanophores: Reactivity and mechanistic insights. *J. Am. Chem. Soc.* **2013**, *135*, 13598–13604.

(54) Wang, J.; Kouznetsova, T. B.; Niu, Z.; Ong, M. T.; Klukovich, H.; Rheingold, A. L.; Martinez, T. J.; Craig, S. L. Inducing and quantifying forbidden reactivity with single-molecule polymer mechanochemistry. *Nat. Chem.* **2015**, *7*, 323–327.
(55) Wang, J.; Kouznetsova, T. B.; Craig, S. L. Single-molecule observation of a mechanically activated *cis*-to-*trans* cyclopropane isomerization. *J. Am. Chem. Soc.* **2016**, *138*, 10410–10412.
(56) Wang, Z.; Kouznetsova, T. B.; Craig, S. L. Pulling outward but reacting inward: Mechanically induced symmetry-allowed reactions of *cis*- and *trans*-diester-substituted dichlorocyclopropanes. *Synlett* **2022**, *33*, 885–889.
(57) Larsen, M. B.; Boydston, A. J. "Flex-activated" mechanophores: Using polymer mechanochemistry to direct bond bending activation. *J. Am. Chem. Soc.* **2013**, *135*, 8189–8192.
(58) Gossweiler, G. R.; Hewage, G. B.; Soriano, G.; Wang, Q.; Welshofer, G. W.; Zhao, X.; Craig, S. L. Mechanochemical activation of covalent bonds in polymers with full and repeatable macroscopic shape recovery. *ACS Macro Lett.* **2014**, *3*, 216–219.
(59) Kabb, C. P.; O'Bryan, C. S.; Morley, C. D.; Angelini, T. E.; Sumerlin, B. S. Anthracene-based mechanophores for compression-activated fluorescence in polymeric networks. *Chem. Sci.* **2019**, *10*, 7702–7708.
(60) Shen, H.; Larsen, M. B.; Roessler, A. G.; Zimmerman, P. M.; Boydston, A. J. Mechanochemical release of *N*-heterocyclic carbenes from flex-activated mechanophores. *Angew. Chem., Int. Ed.* **2021**, *60*, 13559–13563.
(61) Sinninghe Damsté, J. S.; Strous, M.; Rijpstra, W. I. C.; Hopmans, E. C.; Geenevasen, J. A. J.; van Duin, A. C. T.; van Niftrik, L. A.; Jetten, M. S. M. Linearly concatenated cyclobutane lipids form a dense bacterial membrane. *Nature* **2002**, *419*, 708–712.
(62) Strous, M.; Pelletier, E.; Mangenot, S.; Rattei, T.; Lehner, A.; Taylor, M. W.; Horn, M.; Daims, H.; Bartol-Mavel, D.; Wincker, P.; Barbe, V.; Fonknechten, N.; Vallenet, D.; Segurens, B.; Schenowitz-Truong, C.; Médigue, C.; Collingro, A.; Snel, B.; Dutilh, B. E.; Op den Camp, H. J. M.; van der Drift, C.; Cirpus, I.; van de Pas-Schoonen, K. T.; Harhangi, H. R.; van Niftrik, L.; Schmid, M.; Keltjens, J.; van de Vossenberg, J.; Kartal, B.; Meier, H.; Frishman, D.; Huynen, M. A.; Mewes, H. W.; Weissenbach, J.; Jetten, M. S. M.; Wagner, M.; Le Paslier, D. Deciphering the evolution and metabolism of an anammox bacterium from a community genome. *Nature* **2006**, *440*, 790–794.
(63) Mascitti, V.; Corey, E. J. Total synthesis of (±)-pentacycloanammoxic acid. *J. Am. Chem. Soc.* **2004**, *126*, 15664–15665.
(64) Mercer, J. A. M.; Cohen, C. M.; Shuken, S. R.; Wagner, A. M.; Smith, M. W.; Moss, F. R., III; Smith, M. D.; Vahala, R.; Gonzalez-Martinez, A.; Boxer, S. G.; Burns, N. Z. Chemical synthesis and self-assembly of a ladderane phospholipid. *J. Am. Chem. Soc.* **2016**, *138*, 15845–15848.
(65) Hancock, E. N.; Kuker, E. L.; Tantillo, D. J.; Brown, M. K. Lessons in strain and stability: Enantioselective synthesis of (+)-[5]-ladderanoic acid. *Angew. Chem., Int. Ed.* **2020**, *59*, 436–441.
(66) Gleiter, R.; Brand, S. Photochemistry of bridged and unbridged octaalkyl-substituted *syn*-tricyclo[4.2.0.$0^{2,5}$]octa-3,7-diene derivatives. *Chem. Eur. J.* **1998**, *4*, 2532–2538.
(67) Ajami, D.; Hess, K.; Köhler, F.; Näther, C.; Oeckler, O.; Simon, A.; Yamamoto, C.; Okamoto, Y.; Herges, R. Synthesis and properties of the first Möbius annulenes. *Chem. Eur. J.* **2006**, *12*, 5434–5445.

(68) Green, S. A.; Vásquez-Céspedes, S.; Shenvi, R. A. Iron–nickel dual-catalysis: A new engine for olefin functionalization and the formation of quaternary centers. *J. Am. Chem. Soc.* **2018**, *140*, 11317–11324.
(69) Epplin, R. C.; Paul, S.; Herter, L.; Salome, C.; Hancock, E. N.; Larrow, J. F.; Baum, E. W.; Dunstan, D. R.; Ginsburg-Moraff, C.; Fessard, T. C.; Brown, M. K. [2]-Ladderanes as isosteres for *meta*-substituted aromatic rings and rigidified cyclohexanes. *Nat. Commun.* **2022**, *13*, 6056.
(70) Seo, J.; Lee, S. Y.; Bielawski, C. W. Unveiling a masked polymer of dewar benzene reveals *trans*-poly(acetylene). *Macromolecules* **2019**, *52*, 2923–2931.
(71) Wu, B.; Wang, J.; Liu, X.; Zhu, R. Bicyclo[2.2.0]hexene derivatives as a proaromatic platform for group transfer and chemical sensing. *Nat. Commun.* **2021**, *12*, 3680.
(72) Yang, J.; Horst, M.; Romaniuk, J. A. H.; Jin, Z.; Cegelski, L.; Xia, Y. Benzoladderene mechanophores: Synthesis, polymerization, and mechanochemical transformation. *J. Am. Chem. Soc.* **2019**, *141*, 6479–6483.
(73) Yang, J.; Horst, M.; Werby, S. H.; Cegelski, L.; Burns, N. Z.; Xia, Y. Bicyclohexene-*peri*-naphthalenes: Scalable synthesis, diverse functionalization, efficient polymerization, and facile mechanoactivation of their polymers. *J. Am. Chem. Soc.* **2020**, *142*, 14619–14626.
(74) Chen, Z.; Mercer, J. A. M.; Zhu, X.; Romaniuk, J. A. H.; Pfattner, R.; Cegelski, L.; Martinez, T. J.; Burns, N. Z.; Xia, Y. Mechanochemical unzipping of insulating polyladderene to semiconducting polyacetylene. *Science* **2017**, *357*, 475–479.
(75) Boswell, B. R.; Mansson, C. M. F.; Cox, J. M.; Jin, Z.; Romaniuk, J. A. H.; Lindquist, K. P.; Cegelski, L.; Xia, Y.; Lopez, S. A.; Burns, N. Z. Mechanochemical synthesis of an elusive fluorinated polyacetylene. *Nat. Chem.* **2021**, *13*, 41–46.
(76) Beyer, M. K. The mechanical strength of a covalent bond calculated by density functional theory. *J. Chem. Phys.* **2000**, *112*, 7307–7312.
(77) Klein, I. M.; Husic, C. C.; Kovács, D. P.; Choquette, N. J.; Robb, M. J. Validation of the CoGEF method as a predictive tool for polymer mechanochemistry. *J. Am. Chem. Soc.* **2020**, *142*, 16364–16381.
(78) Driessen, P. B. J.; Hogeveen, H. $AlCl_3$ σ complexes of cyclobutadienes. *J. Am. Chem. Soc.* **1978**, *100*, 1193–1200.
(79) Ha, S.; Lee, Y.; Kwak, Y.; Mishra, A.; Yu, E.; Ryou, B.; Park, C. M. Alkyne–alkene [2 + 2] cycloaddition based on visible light photocatalysis. *Nat. Commun.* **2020**, *11*, 2509.
(80) Sun, Y.; Neary, W. J.; Burke, Z. P.; Qian, H.; Zhu, L.; Moore, J. S. Mechanically triggered carbon monoxide release with turn-on aggregation-induced emission. *J. Am. Chem. Soc.* **2022**, *144*, 1125–1129.
(81) Grimme, S. Exploration of chemical compound, conformer, and reaction space with meta-dynamics simulations based on tight-binding quantum chemical calculations. *J. Chem. Theory Comput.* **2019**, *15*, 2847–2862.
(82) Robertson, J.; Pillai, J.; Lush, R. K. Radical translocation reactions in synthesis. *Chem. Soc. Rev.* **2001**, *30*, 94–103.
(83) Stateman, L. M.; Nakafuku, K. M.; Nagib, D. A. Remote C–H functionalization via selective hydrogen atom transfer. *Synthesis* **2018**, *50*, 1569–1586.
(84) Guo, W.; Wang, Q.; Zhu, J. Visible light photoredox-catalysed remote C–H functionalisation enabled by 1,5-hydrogen atom transfer (1,5-HAT). *Chem. Soc. Rev.* **2021**, *50*, 7359–7377.

(85) López, C. S.; Faza, O. N.; de Lera, Á. R. Electrocyclic ring opening of *cis*-bicyclo[*m*.*n*.0]alkenes: The anti-Woodward-Hoffmann quest. *Chem. Eur. J.* **2007**, *13*, 5009–5017.
(86) Lenhardt, J. M.; Ramirez, A. L. B.; Lee, B.; Kouznetsova, T. B.; Craig, S. L. Mechanistic insights into the sonochemical activation of multimechanophore cyclopropanated polybutadiene polymers. *Macromolecules* **2015**, *48*, 6396–6403.
(87) McFadden, M. E.; Overholts, A. C.; Osler, S. K.; Robb, M. J. Validation of an accurate and expedient initial rates method for characterizing mechanophore reactivity. *ACS Macro Lett.* **2023**, *12*, 440–445.